Revision 3

The role of magmatic and hydrothermal processes in the evolution of Be-bearing pegmatites: Evidence from beryl and its breakdown products

SABINA STRMIĆ PALINKAŠ[1], REINHARD WEGNER[2], ANDREA ČOBIĆ[1], LADISLAV A. PALINKAŠ[1], SANDRA DE BRITO BARRETO[3], TAMÁS VÁCZI[4], VLADIMIR BERMANEC[1]

[1] University of Zagreb, Faculty of Science, Geological department, Horvatovac 95, Zagreb, Croatia

[2]Universidad Federal de Campina Grande, Centro de Ciências e Tecnologia, Departamento de Mineração e Geologia, Av. Aprígio Veloso, 882, Bodocongó, Campina Grande, PB, Brazil

[3] Federal University of Pernambuco, Department of Geology, Av. Academico Hélio Ramos. S/N. 5 andar., Cidade Universitária, Recife, PE, Brasil

[4] Eötvös Loránd University, Department of Mineralogy, Pázmány P. sétány 1/C, Budapest, Hungary

ABSTRACT

Beryl and euclase crystals from the Mina do Santino and the Jacú pegmatites in the Borborema Pegmatite Province in northeastern Brazil contain several generations of melt and fluid inclusions, which allow interpretation of P-T-X conditions responsible for beryl crystallization and for alteration of a primary pegmatitic mineral assemblage to a mixture of hydrothermal minerals (euclase, bertrandite, kaolinite and quartz). Primary melt and fluid inclusions hosted by beryl were trapped simultaneously. However, their homogenization temperatures are significantly higher (870-900 °C) than the values previously reported for pegmatitic systems (<712°C) and should to be treat with caution. An isobaric drop of temperature resulted in the exsolution of a fluid. A low-salinity CO_2-enriched phase and a

saline water-rich phase were trapped in pseudosecondary inclusions in beryl at a pressure of 2.1-2.7 kbar and temperature of 390-480 °C. Cooling of the country rocks below 400 °C caused a ductile-to-brittle transition and allowed infiltration of cold groundwater, which further decreased the temperature in the system to 190-240 °C. At the same time, the pressure dropped from a lithostatic (2.1-2.7 kbar) to a hydrostatic value (0.57-0.73 kbar). Consequently, minerals deposited under magmatic conditions (feldspars and beryl) became unstable and a newly-formed hydrothermal mineral paragenesis (euclase, bertrandite, kaolinite and quartz) overprinted the earlier one. The hydrothermal fluids responsible for the alteration differ from the earlier-exsolved fluids in having a lower salinity, lower homogenization temperature, the absence of CO_2 and the presence of CH_4.

Keywords: Mina do Santino, Jacú pegmatite, beryl, euclase, bertrandite, kaolinite, quartz, hydrothermal alterations, fluid and melt inclusions

INTRODUCTION

Beryl is a common mineral in late magmatic and pegmatitic rocks (e.g., Evensen et al., 1999). Although it is a chemically resistant mineral, there are several localities worldwide where beryl was replaced by a mixture of different Be- minerals (e.g. Černý, 1968, 2002). This type of alteration is mostly related to late-magmatic, hydrothermal and metamorphic events (Markl and Schumacher, 1997). Experimental studies of the stability and phase equilibria of Be- minerals in various simplified systems were reviewed by Franz and Morteani (2002). However, there is still some disagreement between experimental data and naturally occurring systems.

At the Mina do Santino and Jacú pegmatites in the Borborema Pegmatite Province (BPP) in northeastern Brazil, beryl is hydrothermally altered to a mixture of euclase, bertrandite,

kaolinite and quartz. Mineral parageneses comprising cogenetic euclase and bertrandite are not common. Euclase has been considered as a Be- phase stable at temperatures and pressures higher than those favorable for bertrandite (Burt, 1978). Furthermore, euclase is stabilized at elevated alumina activities in alkali- and silica-poor environments (Barton 1986; Černý, 2002).

At Borborema, beryl crystallized in the late magmatic stage from granitic melts significantly enriched in incompatible elements and water. During crystallization, it can trap droplets of the original melt and/or coexisting fluid preserved in the form of primary and pseudosecondary inclusions (melt and/or fluid). Consequently, these inclusions provide important information about the magmatic stage of the investigated pegmatites. Secondary inclusions hosted by beryl may represent fluids responsible for the hydrothermal alteration. Euclase, which formed as an alteration product of beryl during the hydrothermal stage, hosts only fluid inclusions. In the present work, comparative studies of melt and fluid inclusions in beryl and fluid inclusions in euclase from the same locality provide valuable information on the magmatic and post-magmatic (hydrothermal) evolution of the investigated pegmatites. We also apply a thermodynamical approach to gain additional insight into the stability of Be-minerals within the P-T-X space.

GEOLOGICAL SETTING

The BPP in northeastern Brazil hosts over 1000 granitic pegmatite bodies (Da Silva et al., 1995; Beurlen et al., 2008). The majority of pegmatites occur in the southeastern part of the BPP within the Seridó Belt of Rio Grande do Norte Tectonic Domain (Fig. 1). Mining activities in the area started during World War I with the exploitation of mica deposits. Subsequently, the area became well-known as one of the world's most important Ta and Be producers, and an important source of raw materials for the ceramics industry and of

gemstones, including aquamarine, morganite and the rare "Paraíba tourmaline" (e.g., Thomas et al., 2011; Beurlen et al., 2011).

The BPP is situated in the west-central part of the Seridó Belt of Pan-African - Brasiliano age, formed during the late Neoproterozoic (ca. 600 Ma) assembly of West Gondwana (Brito Neves et al., 2000). The Seridó Belt represents a metasedimentary sequence that overlies early Paleoproterozoic to Archean basement of the Rio Grande do Norte Domain (Fig. 1). A geological overview of the Seridó Belt was given by Van Schmus et al. (2003). The Seridó Belt comprises a basal volcano-sedimentary sequence (Jucurutu Formation), overlain by quartzites and metaconglomerates (Equador Formation), and an upper turbidite–flysch sequence (Seridó Formation). These rocks were metamorphosed to the upper amphibolite facies (Abukuma type) and locally retrogressively transformed into upper-greenschist facies rocks (Lima, 1986). Jardim de Sá et al. (1981) distinguished four generations of granite intrusions in the area. The formation of the pegmatites is related to granites of the late- to post-orogenic phase (Araújo et al. 2001), known as G4 granites (Jardim de Sá, 1984; Da Silva et al., 1995; Baumgartner et al., 2006). About 80% of the granitic pegmatites in the BPP are hosted by garnet–cordierite and/or sillimanite–biotite schists of the uppermost Seridó Formation. Another 11% of the bodies, including the Mina do Santino and Jacú pegmatites studied here, intruded the underlying quartzites, meta-arkoses and meta-conglomerates of the Equador Formation (Da Silva et al., 1995). The remaining 9% are hosted by gneisses and skarns of the Jucurutú Formation, by late G3 and G4 granites (Jardim de Sá et al., 1981), or by gneisses and migmatites of the Paleoproterozoic basement.

The common feature of the investigated pegmatites is an intensive hydrothermal alteration resulting in complete replacement of feldspars by a mixture of clay minerals, predominately kaolinite. Chemically resistant pegmatite minerals, such as quartz, tourmaline,

columbite and beryl, are at least partly preserved. At both locations, beryl is partly altered to a mixture comprising euclase, bertrandite, kaolinite and quartz.

On the basis of their mineral parageneses, the Jacú and Mina do Santino pegmatites belong to the LCT family (rare-element pegmatites) distinguished by Černý and Ercit (2005). The Jacú pegmatite (6.84°S and 36.69°W) is up to 200 meters wide and hosted by the Neoproterozoic quartzites of the Equador Formation (Fig. 1). Despite the intensive alteration, its zonal structure is partly preserved. The wall zone comprises kaolinite and quartz. The intermediate zone consists mainly of a white kaolinized matrix (Fig. 2) and nests of resistant minerals (tourmaline, columbite, quartz, partly altered beryl). Tantalite, native bismuth and bismuthinite occur locally. The quartz core is fresh and contains both white and rose quartz. According to Ferreira et al. (2008) beryl associated with euclase and clay minerals commonly occurs at the contact between the intermediate zone and the quartz core.

The Mina do Santino pegmatite represents an intensively hydrothermally altered part of the Alto dos Mamões pegmatite, which was described in detail by Da Silva (1993). It is exposed in an underground mine (6.91°S and 36.73°W). Similar to the Jacú pegmatite, clusters of resistant minerals (muscovite, tourmaline, rose quartz, columbite) and partly altered beryl are hosted by a kaolinized matrix.

ANALYTICAL METHODS

Beryl and associated alteration products were separated from the kaolinized matrix for phase analysis. Mineral identification by X-ray powder diffraction was performed on unoriented samples using a Philips PW 3040/60 X'Pert PRO diffractometer (40 kV, 40 μA) with CuK_α monochromatized radiation ($\lambda = 1.54056$ Å) and θ-θ geometry. Samples were scanned between 4 and 65° 2θ with 0.02° step size and a counting time of 1 s per step. The goniometer was calibrated using a quartz standard. Phase identification was performed using

126 the X'Pert Highscore Plus v. 2.1 software (PANalytical, 2004) in combination with Powder
127 Diffraction File 2 (2004).

128 Microthermometric and Raman spectroscopic investigations were carried out on beryl
129 and euclase crystals. Beryl was cut and double-polished into sections about 300 μm in thick.
130 Wafers of euclase approximately 200-300 μm in thick were prepared by cleaving crystals
131 along {010}. Microthermometric measurements of fluid inclusions were conducted using a
132 Linkam THMS 600 stage mounted on an Olympus BX 51 microscope using 10x and 50x
133 Olympus long-working distance objectives. Two synthetic fluid inclusion standards (SYN
134 FLINC; pure H_2O and mixed H_2O-CO_2) were used for calibration. The estimated precision of
135 the measurements was ±2.0 °C for homogenization temperature, and ±0.2 °C in the
136 temperature range between –60 and +10 °C. Melt inclusions were reheated using a Linkam
137 THMS 1500 high-temperature heating stage mounted on a NIKON E600 polarizing
138 microscope equipped with 10x and 50x objectives. The measurements were conducted up to
139 1000 °C under atmospheric pressure. The heating stage was calibrated using the melting
140 temperatures of NaCl (801 °C), Ag (962 °C), Au (1064 °*C)* and Cu (1085 °C).

141 A JobinYvon LabRAM HR800 confocal Raman spectrometer equipped with a frequency
142 doubled Nd-YAG laser (100 mW, 532.2 nm) and a LMPlan FI 100x objective (Olympus) was
143 used to identify volatile and solid phases in inclusions. The identifications were based on
144 Raman spectra provided in the literature (Burke, 2001; Downs, 2006; Frezzotti et al., 2012;
145 Frost et al., 2012).

146 The FLUIDS computer package (Bakker 2003; Bakker and Brown, 2003) was used to
147 calculate fluid properties, including isochores. Calculations were performed in the H_2O–NaCl,
148 H_2O–CO_2-NaCl and H_2O–CH_4-NaCl fluid systems, depending on the estimated fluid
149 inclusion composition.
150

RESULTS

Petrography and Raman spectroscopy of inclusions

Beryl hosts at least three generations of inclusions: primary, pseudosecondary and secondary. The primary inclusions occur in growth zones and clusters, usually have irregular shapes and reach up to 100 μm in size. The primary inclusions can be subdivided into three subgroups: 1) solid; 2) solid-rich melt and 3) fluid-rich inclusions. All of these inclusion types occur together, demonstrating that they represent coexisting phases entrapped during a single crystallization event. The solid inclusions are monophase (Figs. 3a, 3b) and were identified as albite and quartz on the basis of their Raman spectra (Figs. 4a, 4b). Melt inclusions contain variable amounts of solid phases at room temperature (up to 90 vol.%), a vapor bubble and an aqueous solution (Fig. 3c). Raman spectroscopic analyses revealed that glass, phosphates (most probably beryllonite [$NaBePO_4$] and brazilianite [$NaAl_3(PO_4)_2(OH)_4$]), quartz, and a Raman-inactive mineral, possibly halite, are the most common solid phases (Figs. 4c, 4d). The vapor phase contains only water. Fluid-rich primary inclusions generally contain an aqueous solution (L), a vapor phase composed of H_2O, traces of CO_2 and N_2 (Fig. 4e) and a transparent solid phase (S in Fig. 3d). Using Raman spectroscopy, the principal daughter mineral was identified as a phosphate, probably brazilianite.

Pseudosecondary inclusions are grouped in discrete, linear to curved thin trails. These inclusions can be subdivided into two principal groups. The first group contains two liquids [an aqueous solution (L_1) and liquid CO_2 (L_2)] and a vapor phase comprising H_2O, CO_2 and in some cases traces of N_2 (Figs. 3e, 4f). The degree of fill (F) varies between 0.65 and 0.75. The second group of pseudosecondary inclusions comprises an aqueous solution (L), a vapor phase composed of H_2O, traces of CO_2 and N_2, and a transparent Raman-inactive solid (S). Their F value is mostly around 0.9 (Fig. 3f).

Secondary fluid inclusions in beryl occur in healed cracks, exhibit irregular to slightly elongate shape and mostly comprise two phases (liquid and vapor), with the F value between 0.8 and 0.9 (Fig. 3g). Raman spectra of the vapor bubble revealed H_2O, N_2 and CH_4 (Fig. 4g); CO_2 was not detected in these inclusions.

Primary fluid inclusions in euclase occur isolated or as clusters. They contain two phases at room temperature (liquid + vapor), and are up to 50 μm in size, with irregular shapes (Fig. 3h). The liquid phase is an aqueous solution and the vapor bubble comprises a mixture of H_2O, N_2 and CH_4 (Fig. 4h). Like in the secondary inclusions in beryl, CO_2 is absent. Secondary inclusions in euclase lie along curved trails, have irregular shapes and comprise two phases (L+V). Their small size (<10 μm) and low optical contrast between the fluid inclusion and the host mineral preclude any microthermometric measurements.

Fluid and melt inclusion microthermometry

Microthermometric characteristics of fluid inclusions hosted by beryl and euclase from the Mina do Santino and Jacú pegmatites are summarized in Table 1 and Figure 5. Only a limited number of melt inclusions in beryl (n = 8) were homogenized completely during heating experiments. Homogenization mostly involved disappearance of a vapor phase in the temperature range between 875 and 890 °C. The majority of melt inclusions decrepitated below this temperature.

The primary fluid-rich inclusions are characterized by homogenization temperature in the range between 870 and 900 °C involving the simultaneous disappearance of the solid and vapor phases.

Pseudosecondary L+V+S inclusions underwent total homogenization to a liquid phase in the range between 260 to 300 °C. The salt melting temperature between 255 and 290°C suggests a total salinity between 35.0 and 37.4 wt. % NaCl equiv. (Bodnar, 2003). Eutectic

temperature (T_e) around -52 °C indicates the presence of divalent cations such as Ca^{2+} in addition to Na^+ in the solution (Crawford, 1981).

The total homogenization in the L_1+L_2+V type of pseudosecondary fluid inclusions is recorded within the wide range between 320 and 430 °C, with two distinctive peaks around 335 and 410 °C. The final CO_2 melting temperature between -56.2 and -58.0 °C corroborates the Raman evidence that CO_2 is the principal volatile component. Clathrate melting temperatures from 7.9 to 8.5 °C suggest a salinity between 2.9 and 4.1 wt. % NaCl equiv. (Darling, 1991). Homogenization of CO_2 occurs by critical behavior in the narrow range between 30.5 and 31.0 °C. Fluid density, estimated using the equations of state for aqueous-carbonic system (Duschek et al., 1990; Duan et al., 1992; Bakker, 1999), ranges between 0.835 and 0.890 g/cm^3.

Secondary inclusions hosted by beryl share the same microthermometric characteristics as primary inclusions from euclase. Homogenization temperature in both types of inclusions ranges from 165 to 200 °C. Their T_e values around -52 °C suggest a Na-Ca-chloride solution. Secondary inclusions in beryl are characterized by hydrate melting temperatures from -28.2 to -30.0 °C and ice melting temperatures between -12.2 and -8.5 °C, which point to a NaCl/(NaCl+$CaCl_2$) ratio between 0.268 and 0.335 (Oakes et al., 1990) and a salinity between 12.4 and 16.1 wt.% NaCl equiv. (Bodnar, 2003).

Primary fluid inclusions in euclase differ from the secondary inclusions in beryl only slightly. Their hydrohalite melting temperature ranges from -28.0 to -30.7 °C and their ice melting temperature between -12.1 and -8.8 °C corresponds to a salinity of 12.6-16.1 wt.% NaCl equiv. (Bodnar, 2003) and a NaCl/(NaCl+$CaCl_2$) ratio between 0.249 and 0.346 (Oakes et al., 1990).

DISCUSSION

Melt and fluid inclusions provide insight on the composition, volatile content, and the P-T conditions under which the pegmatite crystallized (Lowenstern, 1995). The coexistence of melt and primary fluid inclusions in beryl indicates that at the time of trapping, the pegmatite-forming melt was an emulsion of two immiscible phases (Roedder, 1992). Their homogenizations within the same temperature range (870-900 °C), imply that the melt and primary fluid inclusions represent conjugate melt pairs simultaneously trapped on both sides of a two-melt solvus (e.g., Thomas et al., 2000, 2012; Veksler, 2004). Melt inclusions represent remnants of a silicate melt, whereas primary fluid inclusions, characterized by the presence of phosphates as the principal daughter minerals (brazilianite), represent remnants of a coexisting silicate-poor and phosphorus-enriched phase. The solid inclusions in beryl (quartz, albite) represent crystals entrapped accidentally during the beryl growth.

Whereas Thomas et al. (2000) inferred complete miscibility between silicate melts and hydrous fluids above a critical point of 712 °C and pressure of 1 kbar in the Erzgebirge pegmatite in Germany, the homogenization temperatures measured in the present study are higher than expected. We assume that homogenization of volatile-rich inclusions at temperatures higher than 700 °C and ambient pressure achieved in a microscope-mounted heating stage have to be interpreted with caution because the run time is usually too short to reach equilibrium conditions for the host-inclusion system (Thomas, 1994). Diffusive loss of water can shift the true trapping temperature to significantly higher values. At temperatures >750-800 °C the diffusive loss of water from the inclusions in quartz is very fast. This probably also applies to beryl owing to the presence of channels some 2.6 Å across the structure of this mineral. Therefore, homogenization experiments (see Thomas et al. 2009) at high pressure (e.g., cold-seal pressure vessel or hydrothermal rapid-quench experiments) should be considered in further study. Alternatively, a high concentration of phosphorus may

promote the immiscibility between silicate-rich and silicate-poor phases (Krigman and Krot, 1991; Bogaerts and Schmidt, 2006).

Pseudosecondary inclusions in beryl represent fluids captured under lower T or P conditions. With a drop in T or P, hydrosaline fluid presumably split into two immiscible phases: a H_2O-rich phase with dissolved salts and a CO_2-enriched phase with a lower salt content (e.g., Roedder, 1992). The isochores for the saline aqueous inclusions (salinity = 35.0-37.4 wt.% NaCl equiv., T_H = 260-300 °C) were constructed after the model published by Bodnar (1994). Isochores for the CO_2-enriched low-salinity inclusions (salinity = 2.9-4.1 wt.% NaCl equiv., T_H = 320-430 °C) were calculated according to the equation of state proposed by Bowers and Helgeson (1983) and modified by Bakker (1999). The most representative isochores for both sets of the pseudosecondary inclusions are presented in Figure 6. Assuming the simultaneous capturing of the high-salinity aqueous inclusions and the low-salinity CO_2-enriched inclusions, the intersections of their isochores constraint fluid T and P to the range from 390 to 480 °C and 2.1 to 2.7 kbar, respectively. The lack of aplites in the study areas, as well as the previously published fluid inclusion data from the Borborema Pegmatite Province (Beurlen et al., 2001; Thomas et al., 2011), suggest the pegmatite emplacement under nearly isobaric conditions.

On the basis of fluid inclusion studies of several Be–Ta–Li–Sn-bearing pegmatites in the Province, Beurlen et al. (2001) estimated the P-T conditions during the emplacement of the pegmatites. Their reported T range of 400-580 °C and P around 3.5 kbar are consiste with the regional metamorphic peak, as well as with the known liquidus conditions for rare-element pegmatite crystallization. Thomas et al. (2011) constrained the formation conditions for tantalite-(Mn) from the Alto do Giz pegmatite in the Borborema Pegmatite Province. On the basis of their fluid and melt inclusion study, these authors concluded that water- and alkaline

carbonate-rich fluids and melts are responsible for the transport of Ta and deposition of tantalite-(Mn) at temperatures around 600 °C under a pressure of about 4 kbar.

The Mina do Santino and the Jacú pegmatites differ from the previously studied Be-bearing pegmatites in the Province in showing evidence of intensive hydrothermal alteration, which suggests that their emplacement took place at shallower crustal levels. The pressure estimated in the present study (2.1-2.7 kbar) corresponds to a depth between 5.7 and 7.3 km, assuming a lithostatic regime.

One possible reaction leading to beryl breakdown to a mixture of euclase, bertrandite, kaolinite and quartz is as follows:

$$2\ Be_3Al_2Si_6O_{18} + 4\ H_2O \leftrightarrow 2\ BeAlSiO_4(OH) + Be_4Si_2O_7(OH)_2 + Al_2Si_2O_5(OH)_4 + 6\ SiO_2 \quad (1)$$

(*beryl*) (*euclase*) (*bertrandite*) (*kaolinite*) (*quartz*)

Secondary fluid inclusions in beryl have the same characteristics as the primary inclusions in euclase, suggesting that both represent hydrothermal fluids responsible for the alteration. These inclusions differ from the earlier fluid generations in showing a lower salinity, lower homogenization temperature, the absence of detectable CO_2 and presence of trace amounts of CH_4.

Generally, the origin of water in the hydrothermal post-pegmatitic stage is ambiguous. According to several authors, a contribution of meteoric water should be considered (e.g., Campbell et al., 1995; Bakker and Elburg, 2006; Piilonen et al., 2012).

The mixing of magmatic water with groundwater is plausible, especially keeping in mind the shallow emplacement position of the investigated pegmatites. Although the studied pegmatites do not show any structural evidence for a brittle-ductile transition, such evidence has been presented for several hydrothermally unaltered pegmatites within the Seridó Belt (Araújo et al., 2001; Baumgartner et al., 2006). At temperatures above 400 °C the country rocks behave in a ductile fashion, sealing the system from significant infiltration of connate

and meteoric waters. Brittle deformation below 400 °C can result in infiltration of groundwater into the system and a transition from lithostatic to hydrostatic pressure (Fournier, 1992). Assuming an emplacement depth between 5.7 and 7.3 km, estimated from the pseudosecondary fluid inclusion data, the hydrostatic pressure in the system would be between 0.53 and 0.73 kbar. The intersection of isochores constructed for the secondary fluid inclusions hosted by beryl and the primary fluid inclusions in euclase with the estimated hydrostatic pressure suggests that the hydrothermal alteration occurred in the temperature interval between 190 and 240 °C (Fig. 6). This agrees well with the P-T curve for reaction (1).

The P-T stability fields for beryl and the mixture of its hydrothermal alteration products, constructed from the thermodynamic data for the BeO-Al_2O_3-SiO_2-H_2O system published by Barton (1986) and Hemingway et al. (1986), are shown in Figure 7.

The primary inclusions in beryl reveal crystallization from a heterogeneous melt and fluid system, which is commonly proposed for the late-stage evolution of granitic magmas (e.g., Roedder 1984; Bakker and Elburg, 2006). According to the microthermometric data, beryl crystallized at T between 870 and 900 °C, but this estimate should be considered with caution owing to the possible diffusive loss of water during our heating experiments. Isobaric cooling of the system resulted in fluid immiscibility and separation of a low-salinity CO_2-rich phase and a highly saline aqueous fluid. Finally, cooling of the country rocks below 400 °C caused a transition from the ductile to brittle regime and allowed infiltration of cold ground water into the system, which further decreased its temperature. Simultaneously, pressure dropped from lithostatic (2.1-2.7 kbar) to hydrostatic (0.57-0.73 kbar) and the system crossed from the stability field of beryl into that of euclase, bertrandite, kaolinite and quartz.

IMPLICATIONS

Numerous recent publications deal with the genesis of pegmatite worldwide (e.g. Beurlen et al., 2011; London and Morgan, 2012; McKechnie et al., 2012) but the key factors responsible for the pegmatite formation and the differences between fertile and sterile granites and pegmatites still have not been unanimously accepted. The open questions involve the role of water and fluxes (e.g. Burnham and Nekvasil, 1986; London et al., 1989; London, 1990; Nabelek et al., 2010; Thomas and Davidson, 2012), the influence of pegmatite–wall rock interactions (e.g. London, 1990; Fuertes-Fuente et al., 2000; Trumbull et al., 2013) and the importance of the brittle-ductile transition in the pegmatite-forming processes (e.g. Brisbin, 1986; Pennacchioni, 2005). The principal implication of this paper is to contribute to the elucidation of some of the questions mentioned above, based on melt and fluid inclusion data in intensively hydrothermally altered pegmatites of the BPP, in northeastern Brazil.

The primary melt and fluid-rich inclusions in beryl record parental melt compositions at the time of host mineral growth. The presence of water (vapor phase in the melt inclusions, liquid and vapor phases in the fluid-rich inclusions) and phosphates (beryllonite, brazilianite) in both types of inclusions indicates that P in addition to H_2O play a significant role in the formation of the investigated pegmatites.

Pseudosecondary inclusions in beryl record a post-crystallization fluid immiscibility between high-saline H_2O-rich and low-saline CO_2-rich fluids. Intersections of their representative isochores allow estimation of the entrapment pressure and calculation of the depth at which the pegmatites were formed.

Secondary inclusions in beryl and primary inclusions in euclase host hydrothermal fluids responsible for the intensive alteration processes. The alteration processes are attributed to a relatively shallow emplacement of the pegmatites and the brittle-ductile transition which moved the system from the lithostatic into hydrostatic regime, decreased the pressure and allowed infiltration of cold groundwater. Except in the investigated pegmatites, the brittle-

ductile transition has been described as a key factor in the deposition of economically important minerals in wide spectrum of hydrothermal ore deposits. (e.g. Lindsay et al., 1995; Strmić Palinkaš et al., 2013; Japas et al., 2013).

From a mineralogical point of view this study implies the cogenetic origin of euclase and bertrandite which have been earlier considered as Be-minerals which do not form under same P-T-X conditions (e.g. Černý, 2002).

Acknowledgments

This study was supported by the by the Croatian Ministry of Sciences, Technology and Sports (Projects No. 119-0000000-1158 and 119-0982709-1175). The authors thank Prof. Csaba Szabó (Lithosphere Fluid Research Laboratory, Eötvös Lorand University, Budapest) for providing access to the equipment for melt inclusion microthermometry, as well as for valuable comments and suggestions. Editorial comments from Anton Chakhmouradian, and detailed and constructive reviews by Robert Trumbull, Rainer Thomas and an anonymous referee helped to improve the manuscript and are greatly appreciated.

REFERENCES

Araújo, M.N.C., da Silva, F.C.A., and de Sá, E.F.J. (2001) Pegmatite Emplacement in the Seridó Belt, Northeastern Brazil: Late Stage Kinematics of the Brasiliano Orogen. Gondwana Research, 4(1), 75-85.

Bakker, R.J. (1999) Adaptation of the Bowers and Helgeson (1983) equation of state to the H_2O–CO_2–CH_4–N_2–NaCl system. Chemical Geology, 154(1–4), 225-236.

Bakker, R.J. (2003) Package FLUIDS 1. Computer programs for analysis of fluid inclusion data and for modeling bulk fluid properties. Chemical Geology, 194(1–3), 3-23.

Bakker, R.J., and Brown, P.E. (2003) Computer modeling in fluid inclusion research. In I. Samson, A. Anderson, and D. Marshall, Eds. Fluid inclusions, analysis and interpretation, 32, p. 175–212. Mineralogical Association of Canada, Ottawa.

Bakker, R., and Elburg, M. (2006) A magmatic-hydrothermal transition in Arkaroola (northern Flinders Ranges, South Australia): from diopside–titanite pegmatites to hematite–quartz growth. Contributions to Mineralogy and Petrology, 152(5), 541-569.

Barton, M.D. (1986) Phase equilibria and thermodynamic properties of minerals in the BeO-Al_2O_3-SiO_2-H_2O (BASH) system, with petrologic applications. American Mineralogist, 71(3-4), 277-300.

Baumgartner, R., Romer, R.L., Moritz, R., Sallet, R., and Chiaradia, M. (2006) Columbite–tantalite-bearing granitic pegmatites from the Seridó Belt, northeastern Brazil: Genetic constraints from U–Pb dating and Pb isotopes. The Canadian Mineralogist, 44(1), 69-86.

Beurlen, H., Da Silva, M.R.R., and de Castro, C. (2001) Fluid inclusion microthermometry in Be–Ta–(Li–Sn)-bearing pegmatites from the Borborema Province, Northeast Brazil. Chemical Geology, 173(1–3), 107-123.

Beurlen, H., Da Silva, M.R., Thomas, R., Soares, D., and Olivier, P. (2008) Nb–Ta–(Ti–Sn) oxide mineral chemistry as tracer of rare-element granitic pegmatite fractionation in the Borborema Province, Northeastern Brazil. Mineralium Deposita, 43(2), 207-228.

Beurlen, H., de Moura, O.J.M., Soares, D.R., da Silva, M.R.R., and Rhede, D. (2011) Geochemical and geological controls on the genesis of gem-quality "Paraíba Tourmaline" in granitic pegmatites from northeastern Brazil. The Canadian Mineralogist, 49(1), 277-300.

Bodnar, R.J. (1994) Synthetic fluid inclusions: XII. The system H_2O-NaCl. Experimental determination of the halite liquidus and isochores for a 40 wt% NaCl solution. Geochimica et Cosmochimica Acta, 58(3), 1053-1063.

Bodnar, R.J. (2003) Reequilibration of fluid inclusions. In I. Samson, A. Anderson, and D. Marshall, Eds. Fluid inclusions, analysis and interpretation, 32, p. 213-230. Mineralogical Association of Canada, Ottawa.

Bogaerts, M., and Schmidt, M.W. (2006) Experiments on silicate melt immiscibility in the system Fe_2SiO_4–$KAlSi_3O_8$–SiO_2–CaO–MgO–TiO_2–P_2O_5 and implications for natural magmas. Contributions to Mineralogy and Petrology, 152(3), 257-274.

Bowers, T.S., and Helgeson, H.C. (1983) Calculation of the thermodynamic and geochemical consequences of nonideal mixing in the system H_2O-CO_2-NaCl on phase relations in geologic systems: Equation of state for H_2O-CO_2-NaCl fluids at high pressures and temperatures. Geochimica et Cosmochimica Acta, 47(7), 1247-1275.

Brisbin, W.C. (1986) Mechanics of pegmatite intrusion. American Mineralogist, 71(3-4), 644-

671.

Brito Neves, B.B., dos Santos, E.J., and Van Schmus, W.R. (2000) Tectonic history of the Borborema Province, northeastern Brazil. In: U. Cordani, E.J. Milani, A. Thomaz Filho, and D.A. Campos, Eds. Tectonic Evolution of South America. Proceedings of the 31st International Geological Congress, Rio de Janeiro, Brazil, p. 151–182.

Burke, E.A.J. (2001) Raman microspectrometry of fluid inclusions. Lithos, 55(1–4), 139-158.

Burnham, C.W., and Nekvasil, H. (1986) Equilibrium properties of granite pegmatite magmas. American Mineralogist, 71(3-4), 239-263.

Burt, D.M. (1978) Multisystems analysis of beryllium mineral stabilities; the system BeO-Al_2O_3-SiO_2-H_2O. American Mineralogist, 63(7-8), 664-676.

Campbell, A.R., Banks, D.A., Phillips, R.S., and Yardley, B.W.D. (1995) Geochemistry of Th-U-REE mineralizing magmatic fluids, Capitan Mountains, New Mexico. Economic Geology, 90(5), 1271-1287.

Crawford, M.L. (1981) Phase equilibria in aqueous fluid inclusions. Fluid inclusions, applications to petrology, 6, p. 75-100. Mineralogical Association of Canada, Calgary.

Charoy, B., de Donato, P., Barres, O., and Pinto-Coelho, C. (1996) Channel occupancy in an alkali-poor beryl from Serra Branca (Goias, Brazil): Spectroscopic characterization. American Mineralogist, 81(3-4), 395-403.

Černý, P. (1968) Beryllumwandlungen in Pegmatiten: Verlauf und Produkte. Neues Jahrbuch für Mineralogie - Abhandlungen, 108, 166-180.

Černý, P. (2002) Mineralogy of Beryllium in Granitic Pegmatites. Reviews in Mineralogy and Geochemistry, 50(1), 405-444.

Černý, P., and Ercit, S. (2005) The classification of granitic pegmatites revisited. The Canadian Mineralogist, 43(6), 2005-2026.

Darling, R.S. (1991) An extended equation to calculate NaCl contents from final clathrate melting temperatures in H_2O-CO_2-NaCl fluid inclusions: Implications for P-T isochore location. Geochimica et Cosmochimica Acta, 55(12), 3869–3871.

Da Silva, M.R.R. (1993) Petrographical and geochemical investigation of pegmatites in the Borborema Pegmatitic Province of Northeast Brazil. Ludwig-Maximilian Universität, PhD thesis, p. 305. Ludwig-Maximilian Universität, München.

Da Silva, M.R.R., Höll, R., and Beurlen, H. (1995) Borborema Pegmatitic Province: geological and geochemical characteristics. Journal of South American Earth Sciences, 8(3–4), 355-364.

Downs, R.T. (2006) The RRUFF Project: an integrated study of the chemistry, crystallography, Raman and infrared spectroscopy of minerals. Program and Abstracts of the 19th General Meeting of the International Mineralogical Association in Kobe, Japan. O03-13

Duan, Z., Möller, N., and Weare, J.H. (1992) An equation of state for the CH_4-CO_2-H_2O system: II. Mixtures from 50 to 1000 °C and 0 to 1000 bar. Geochimica et Cosmochimica Acta, 56(7), 2619–2631.

Duschek, W., Kleinrahm, R., and Wagner, W. (1990) Measurements and correlation of the (pressure, density, temperature) relation of carbon dioxide: II. Saturated-liquid and saturated-vapour densities and the vapour pressure along the entire coexistence curve. Journal of Chemical Thermodynamics, 22(9), 841–864.

Evensen, J.M., London, D., and Wendlandt, R.F. (1999) Solubility and stability of beryl in granitic melts. American Mineralogist, 84(5-6), 733-745.

Ferreira, A.C.M., Ferreira, J.A. de M., Soares, D.R., and Tavares, J.F. (2008) Ocorrências de euclásios gemas em pegmatitos berilo-tantalíferos da região do Seridó, Província Pegmatítica da Borborema. Estudos Geológicos, 18(2), 117-128.

Fournier, R.O. (1992) The influences of depth of burial and the brittle-ductile transition on the evolution of magmatic fluids. Geological Survey of Japan Report, 277, 57-59.

Franz, G., and Morteani, G. (2002) Be-minerals: synthesis, stability, and occurrence in metamorphic rocks. Reviews in Mineralogy and Geochemistry, 50(1), 551-589.

Frezzotti, M.L., Tecce, F., and Casagli, A. (2012) Raman spectroscopy for fluid inclusion analysis. Journal of Geochemical Exploration, 112, 1-20.

Frost, R.L., Xi, Y., Scholz, R., Belotti, F.M., and Alberto Dias Menezes Filho, L. (2012) Raman and infrared spectroscopic characterization of beryllonite, a sodium and beryllium phosphate mineral – implications for mineral collectors. Spectrochimica Acta Part A: Molecular and Biomolecular Spectroscopy, 97, 1058-1062.

Fuertes-Fuente, M., Martin-Izard, A., Boiron, M.C., and Viñuela, J.M. (2000) P–T path and fluid evolution in the Franqueira granitic pegmatite, central Galicia, Northwestern Spain. The Canadian Mineralogist, 38(5), 1163-1175.

Hemingway, B.S., Barton, M.D., Robie, R.A., and Haselton, H.T. (1986) Heat capacities and thermodynamic functions for beryl, $Be_3Al_2S_{i6}O_{18}$, phenakite, Be_2SiO_4 , euclase, $BeAlSiO_4(OH)$, bertrandite, $Be_4Si_2O_7(OH)_2$, and chrysoberyl, $BeAl_2O_4$. American Mineralogist, 71(3-4), 557-568.

Japas, M.S., Rubinstein, N.A., and Kleiman, L.E. (2013) Strain Fabric Analysis applied to

hydrothermal ore deposits emplaced during changing geodynamical conditions (Infiernillo and Las Picazas, San Rafael Massif, Argentina). Ore Geology Reviews, 53(1), 357-372.

Jardim de Sá, E.F. (1994) A Faixa Seridó (Província Borborema, NE do Brasil) e seu significado geodinâmico na cadeia Brasiliana/Panafricana. University of Brasilia, p. 762. University of Brasilia, Brasilia.

Jardim de Sá, E.F., Legrand, J.M., and McReath, I. (1981) Estratigrafia de rochas granitóides na Região do Seridó (RN-PB) com base em critérios estruturais. Revista Brasileira de Geociências, 11, 50-57.

Krigman, L.D., and Krot, T.V. (1991) Stable phosphate aluminosilicate liquation in magmatic melts. Geokhimiya, 11, 1548–1560 (in Russian).

Lima, E.S. (1986) Metamorphism and tectonic evolution in the Seridó Region, Northeastern Brazil. University of California, PhD thesis, p. 215. University of California, Los Angeles.

Lindsay, D.D., Zentilli, M., and Rivera, J.R.D.L. (1995) Evolution of an active ductile to brittle shear system controlling mineralization at the Chuquicamata porphyry copper deposit, northern Chile. International Geology Review, 37(11), 945-958.

London, D. (1990) Internal differentiation of rare-element pegmatites; a synthesis of recent research. Geological Society of America Special Papers, 246, 35-50.

London, D., and Morgan, G.B. (2012) The pegmatite puzzle. Elements, 8(4), 263-268.

London, D., Morgan, G. B., and Hervig, R. L. (1989) Vapor-undersaturated experiments with Macusani glass + H_2O at 200 MPa, and the internal differentiation of granitic pegmatites. Contributions to Mineralogy and Petrology, 102(1), 1-17.

Lowenstern, J. B. (1995) Applications of silicate-melt inclusions to the study of magmatic volatiles. In Thompson J. F. H., Ed., Magmas, Fluids, and Ore Deposits, 23, p. 71-100, Mineral. Mineralogical Association of Canada Short Course.

Markl, G., and Schumacher, J.C. (1997) Beryl stability in local hydrothermal and chemical environments in a mineralized granite. American Mineralogist, 82(1-2), 194-202.

McKechnie, C.L., Annesley, I.R., and Ansdell, K.M. (2012). Medium-to low-pressure pelitic gneisses of Fraser Lakes Zone B, Wollaston Domain, Northern Saskatchewan, Canada: mineral compositions, metamorphic P–T–t path, and implications for the genesis of radioactive abyssal granitic pegmatites. The Canadian Mineralogist, 50(6), 1669-1694.

Nabelek, P.I., Whittington, A.G., and Sirbescu, M.L.C. (2010). The role of H_2O in rapid

emplacement and crystallization of granite pegmatites: resolving the paradox of large crystals in highly undercooled melts. Contributions to Mineralogy and Petrology, 160(3), 313-325.

Oakes C.S., Bodnar R.J., and Simonson J.M. (1990) The system NaCl–$CaCl_2$–H_2O: I. The ice liquidus at 1 atm total pressure. Geochimica et Cosmochimica Acta, 54(3), 603-610.

PANalytical (2004) X'Pert Highscore Plus version 2.1. PANalytical, Almelo, Netherlands.

Pennacchioni, G. (2005) Control of the geometry of precursor brittle structures on the type of ductile shear zone in the Adamello tonalites, Southern Alps (Italy). Journal of Structural Geology, 27(4), 627-644.

Piilonen, P.C., McDonald, A.M., Poirier, G., Rowe, R., and Larsen, A.O. (2012) The mineralogy and crystal chemistry of alkaline pegmatites in the Larvik plutonic complex, Oslo rift valley, Norway. Part 1. Magmatic and secondary zircon; implications for petrogenesis from trace-element geochemistry. Mineralogical Magazine, 76(3), 649–672.

Powder Diffraction File 2 (2004): Database Sets 1-54. International Centre for Diffraction data (ICSS), Newton Square, Pennsylvania.

Roedder, E. (1984) Fluid inclusions. Reviews in Mineralogy, 12, 644 p.

Roedder, E. (1992) Fluid inclusion evidence for immiscibility in magmatic differentiation. Geochimica et Cosmochimica Acta, 56(1), 5-20.

Strmić Palinkaš, S., Palinkaš, L.A., Renac, C., Spangenberg, J.E., Lüders, V., Molnar, F., and Maliqi, G. (2013) Metallogenic Model of the Trepča Pb-Zn-Ag Skarn Deposit, Kosovo: Evidence from Fluid Inclusions, Rare Earth Elements, and Stable Isotope Data. Economic Geology, 108(1), 135-162.

Thomas, R. (1994) Estimation of the viscosity and the water content of silicate melts from melt inclusion data. European Journal of Mineralogy, 6(4), 511-535.

Thomas, R., and Davidson, P. (2012) Water in granite and pegmatite-forming melts. Ore Geology Reviews, 46(1), 32-46.

Thomas, R., Webster, J.D., and Heinrich, W. (2000) Melt inclusions in pegmatite quartz: complete miscibility between silicate melts and hydrous fluids at low pressure. Contributions to Mineralogy and Petrology, 139(4), 394-401.

Thomas, R., Davidson, P., Rhede, D., and Leh, M. (2009) The miarolitic pegmatites from the Königshain: a contribution to understanding the genesis of pegmatites. Contribution to Mineralogy and Petrology, 157(4), 505-523.

Thomas, R., Davidson, P., and Beurlen, H. (2011) Tantalite-(Mn) from the Borborema

Pegmatite Province, northeastern Brazil: conditions of formation and melt- and fluid-inclusion constraints on experimental studies. Mineralium Deposita, 46(7), 749-759.

Thomas, R, Davidson, P., and Beurlen, H. (2012) The competing models for the origin and internal evolution of granitic pegmatites in the light of melt and fluid inclusion research. Mineralogy and Petrology, 106(1-2), 55-73.

Trumbull, R.B., Beurlen, H., Wiedenbeck, M., and Soares, D.R. (2013) The diversity of B-isotope variations in tourmaline from rare-element pegmatites in the Borborema Province of Brazil. Chemical Geology, 352(1), 47-62.

Van Schmus, W.R., Brito Neves, B.B., Williams, I.S., Hackspacher, P., Fetter, A.H., Dantas, E.L., and Babinski, M. (2003) The Seridó Group of NE Brazil, a late Neoproterozoic pre- to syn-collisional basin in West Gondwana: insights from SHRIMP U–Pb detrital zircon ages and Sm–Nd crustal residence (TDM) ages. Precambrian Research, 127, 287–327.

Veksler, I.V. (2004) Liquid immiscibility and its role at the magmatic-hydrothermal transition: a summary of experimental studies. Chemical Geology, 210, 7-31.

Wood, D.L., and Nassau, K. (1968) The characterization of beryl and emerald by visible and infrared absorption spectroscopy. American Mineralogist, 53, 777-800.

Figure captions:

Fig. 1. Regional geologic setting of the Mina do Santina and Jacu pegmatites within the Seridó Foldbelt (after Jardim de Sá et al., 1981). Tur – tourmaline, Kln – kaolinite, Fds – feldspar, gem – gemstone.

Fig. 2. a) The hydrothermally altered Jacu pegmatite body. The resistant minerals (tourmaline, columbite, quartz, partly altered beryl and its alteration products) are hosted by the white kaolinitized matrix; **b)** Hydrothermally altered beryl with the alteration products, the Mina do Santina pegmatite.

Fig. 3. Microphotographs of **a)** Solid albite (Ab) inclusion in beryl, the Jacu pegmatite; **b)** Solid quartz (Qtz) inclusion hosted by beryl, the Jacu pegmatite; **c)** Melt inclusion in beryl has numerous distinctive solid phases (Qtz – quartz, Gls – glass, Ber – beryllonite), the Mina do Santina pegmatite; **d)** An example of the primary fluid

inclusion in beryl consisting of liquid, vapor and solid phases, the Jacu pegmatite. The solid phase usually is brazilianite (Brz); **e)** Pseudosecondary fluid inclusion from beryl comprising two immiscible liquids (L_1, L_2) and vapor (V) phase, the Mina do Santina pegmatite; **f)** An example of the pseudosecondary fluid inclusion from beryl comprising liquid, vapor and solid phase, the Mina do Santina pegmatite; **g)** Secondary fluid inclusions in beryl, the Mina do Santina pegmatite; **h)** Primary fluid inclusions in euclase, the Mina do Santina pegmatite.

Fig. 4. Raman spectra of **a)** Albite solid inclusion hosted by beryl, the Jacu pegmatite; **b)** Quartz solid inclusion in beryl,the Jacu pegmatite; **c)** Solid phosphate phase, probably beryllonite, in a melt inclusion from beryl, the Mina do Santina pegmatite; **d)** Solid phosphate phase, probably brazilianite, in a melt inclusion from beryl, the Jacu pegmatite; **e)** A vapor phase from a typical primary fluid-phases rich inclusion hosted by beryl, the Mina do Santina pegmatite; **f)** A vapor phase from a L_1+L_2+V pseudosecondary fluid inclusion in beryl, the Mina do Santina pegmatite; **g)** A vapor phase from a typical secondary fluid inclusion in beryl, the Jacu pegmatite, contains traces of CH_4 and N_2; **h)** A vapor phase from a typical primary fluid inclusion hosted by euclase, the Jacu pegmatite, contains CH_4 and N_2.
The band at 688 cm^{-1} and 256 cm^{-1} corresponds to the host beryl (Brl) and euclase (Eu), respectively. The sharp bands at 3597 and 3606 cm^{-1} corresponds to the stretching of isolated H_2O molecules accommodated in the vacant channels of beryl (Wood and Nassau, 1968; Charoy et al., 1996).

Fig. 5. Frequency distribution of **a)** salinity; **b)** total homogenization temperature

Fig. 6. Pressure–temperature diagram showing the isochores for the most representative fluid inclusion types hosted by beryl and euclase from the Mina do Santina and Jacu pegmatites. Isochores 1 and 2 represent the pseudosecondary L_1+L_2+V fluid inclusion type from beryl. Isochores 3 and 4 correspond to the pseudosecondary L+V+S fluid inclusion type from beryl. Isochores 5 and 6 represent the secondary fluid inclusions from beryl as well as the primary fluid inclusions hosted by euclase.

Fig. 7. Pressure–temperature diagram showing the stability fields of beryl and the recorded hydrothermal alteration products. Estimated P-T conditions of the crystallization and

613 the break-down of beryl from the Mina do Santina and Jacu pegmatites are
614 superimposed.
615
616
617
618

Table 1. Summary of inclusion types from the Mina do Santina and Jacu pegmatites, the Borborema Pegmatitic Province, northeastern Brazil.

Host mineral	Inclusion type	Genetic type	Composition	Microthermometric data										State	n
				T_{clath} (°C)		$T_{m\ ice}$ (°C)		T_S (°C)		Salinity (wt.%. NaCl equ.)		T_H (°C)			
				Range	Mdn ± σ	Range	Mdn ± σ	Range	Mdn ± σ	Range	Mdn ± σ	Range	Mdn ± σ		
Beryl	Solid inclusions (SI)	Primary	Qtz, Ab												
	Melt inclusions (MI)	Primary	G, Bry, Bra, Qtz, Hl, H_2O									875-890	884 ± 7	M	8
	Fluid inclusions (L+V+S)	Primary	H_2O, ±CO_2, ±N_2, Bra					870-900	873 ± 10			870-900	877 ± 7	L	15
	Fluid inclusions (L+V+S)	Pseudosecondary	H_2O, ±CO_2, ±N_2, Hl					255-290	268 ± 12	35.0-37.4	36.4 ± 0.7	260-300	275 ± 11	L	25
	Fluid inclusions (L_1+L_2+V)	Pseudosecondary	H_2O, CO_2, ±N_2	7.9-9.0	8.2 ± 0.2					2.9-4.1	3.5 ± 0.4	320-430	376 ± 41	L	35
	Fluid inclusions (L+V)	Secondary	H_2O, ±CH_4, ±N_2			-12.2 to -8.5	-11.0 ± 1.2			12.4-16.2	15.0 ± 1.3	165-200	177 ± 10	L	25
Euclase	Fluid inclusions (L+V)	Primary	H_2O, ±CH_4, ±N_2			12.1 to -8.8	-10.7 ± 1.1			12.6-16.1	14.7 ± 1.1	165-200	185 ± 13	L	25

Qtz – quartz, Ab – albite, G – glass, Bry – beryllonite, Bra – brazilianite, Hl – halite.
T_{clath} – clathrate melting temperature, $T_{m\ ice}$ – ice melting temperature, T_S – salt dissolution temperature, T_H – homogenization temperature.
M – melt, L – liquid, V – vapor .
Mdn – median, σ – standard deviation, n – total number of the microthermometric measurements.

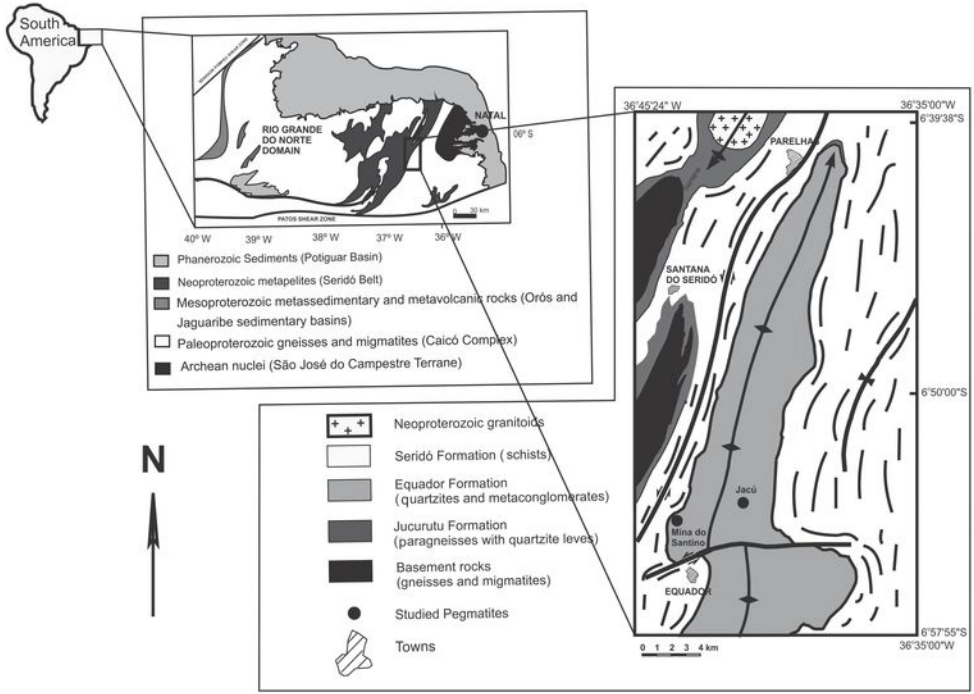
South America
RIO GRANDE DO NORTE DOMAIN
NATAL
06° S
PATOS SHEAR ZONE
0 30 km
40° W
39° W
38° W
37° W
36° W
Phanerozoic Sediments (Potiguar Basin)
Neoproterozoic metapelites (Seridó Belt)
Mesoproterozoic metassedimentary and metavolcanic rocks (Orós and Jaguaribe sedimentary basins)
Paleoproterozoic gneisses and migmatites (Caicó Complex)
Archean nuclei (São José do Campestre Terrane)
36°45'24" W
36°35'00"W
6°39'38"S
PARELHAS
SANTANA DO SERIDÓ
6°50'00"S
Jacú
Mina do Santino
EQUADOR
6°57'55"S
36°35'00"W
0 1 2 3 4 km
N
Neoproterozoic granitoids
Seridó Formation (schists)
Equador Formation (quartzites and metaconglomerates)
Jucurutu Formation (paragneisses with quartzite leves)
Basement rocks (gneisses and migmatites)
Studied Pegmatites
Towns

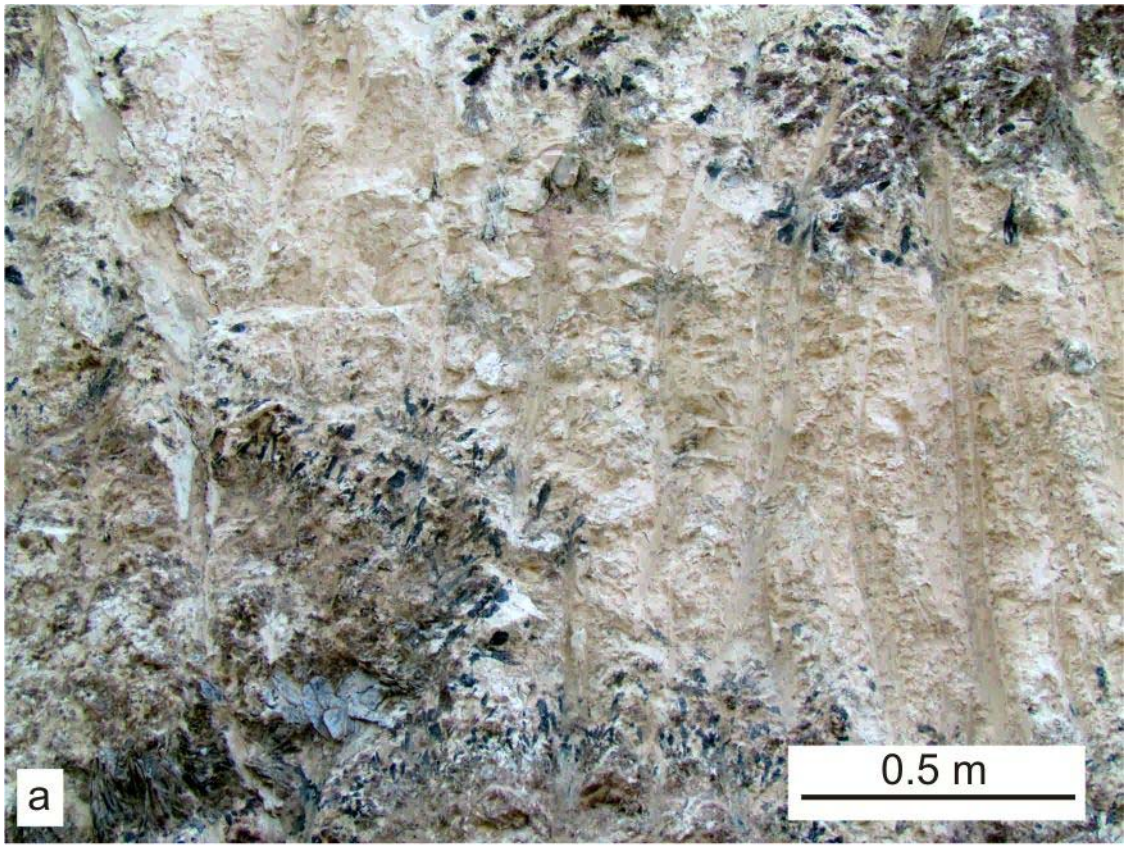
a
0.5 m


Eu + Bert + Kln + Qtz
Brl
Brl
Brl
b
1 cm

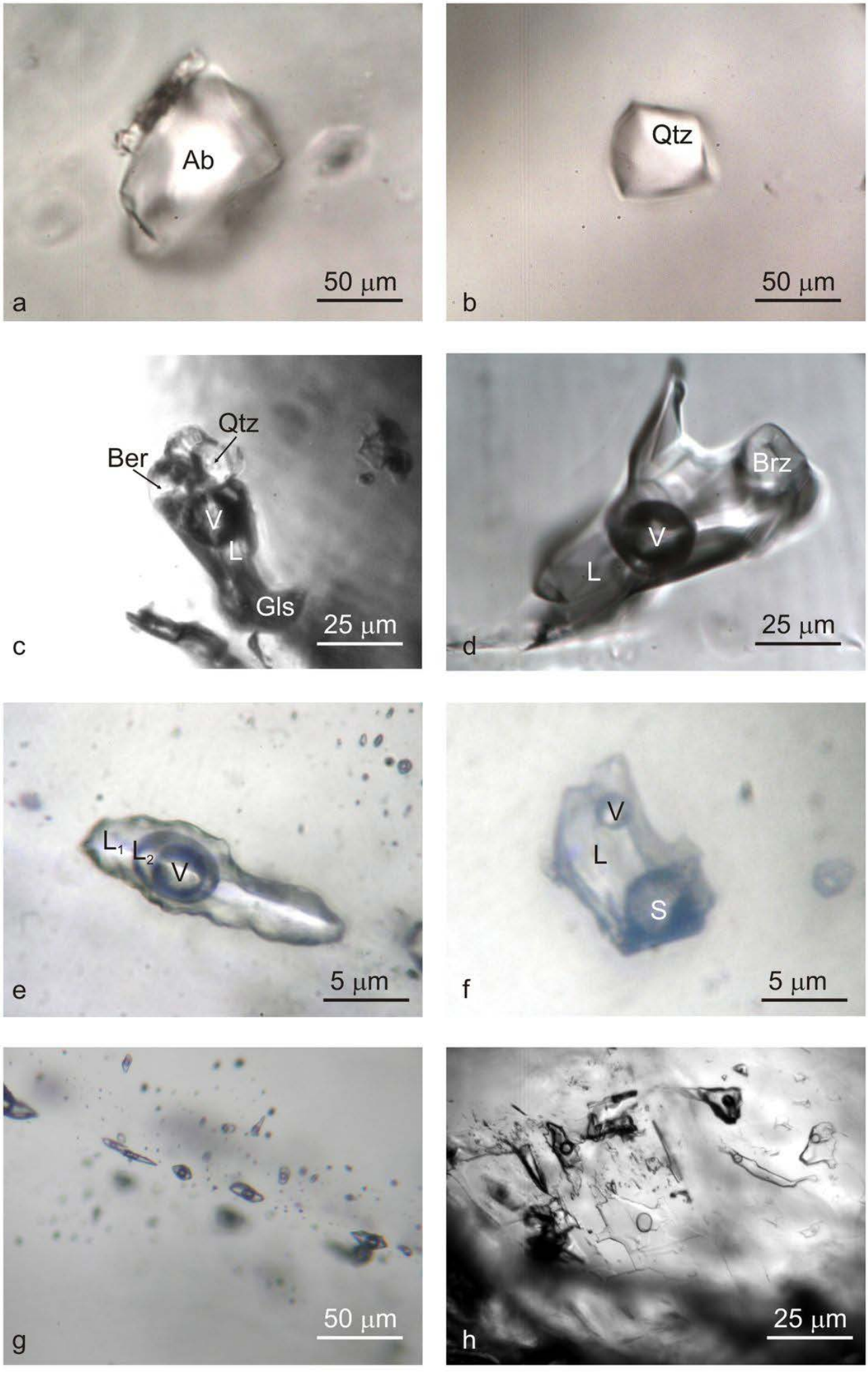
Ab
50 μm
a
Qtz
50 μm
b
Qtz
Ber
V
L
Gls
25 μm
c
Brz
V
L
25 μm
d
L1 L2
V
5 μm
e
V
L
S
5 μm
f
50 μm
g
25 μm
h

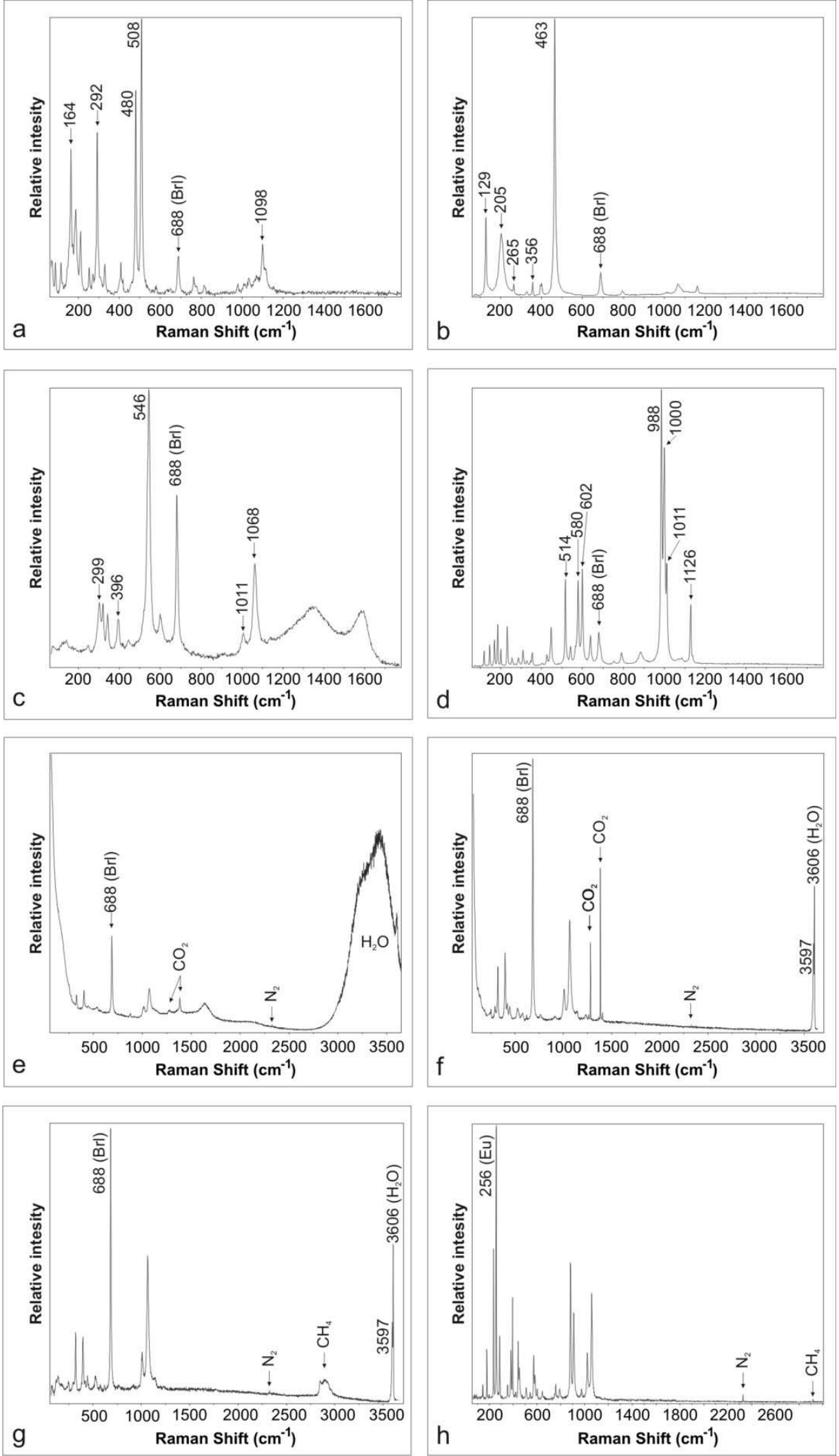
a
Relative intesity
164
292
480
508
688 (Brl)
1098
200 400 600 800 1000 1200 1400 1600
Raman Shift (cm-1)
b
Relative intesity
129
205
265
356
463
688 (Brl)
200 400 600 800 1000 1200 1400 1600
Raman Shift (cm-1)
c
Relative intesity
299
396
546
688 (Brl)
1011
1068
200 400 600 800 1000 1200 1400 1600
Raman Shift (cm-1)
d
Relative intesity
514
580
602
688 (Brl)
988
1000
1011
1126
200 400 600 800 1000 1200 1400 1600
Raman Shift (cm-1)
e
Relative intesity
688 (Brl)
CO2
N2
H2O
500 1000 1500 2000 2500 3000 3500
Raman Shift (cm-1)
f
Relative intesity
688 (Brl)
CO2
CO2
N2
3597
3606 (H2O)
500 1000 1500 2000 2500 3000 3500
Raman Shift (cm-1)
g
Relative intesity
688 (Brl)
N2
CH4
3597
3606 (H2O)
500 1000 1500 2000 2500 3000 3500
Raman Shift (cm-1)
h
Relative intesity
256 (Eu)
N2
CH4
200 600 1000 1400 1800 2200 2600
Raman Shift (cm-1)

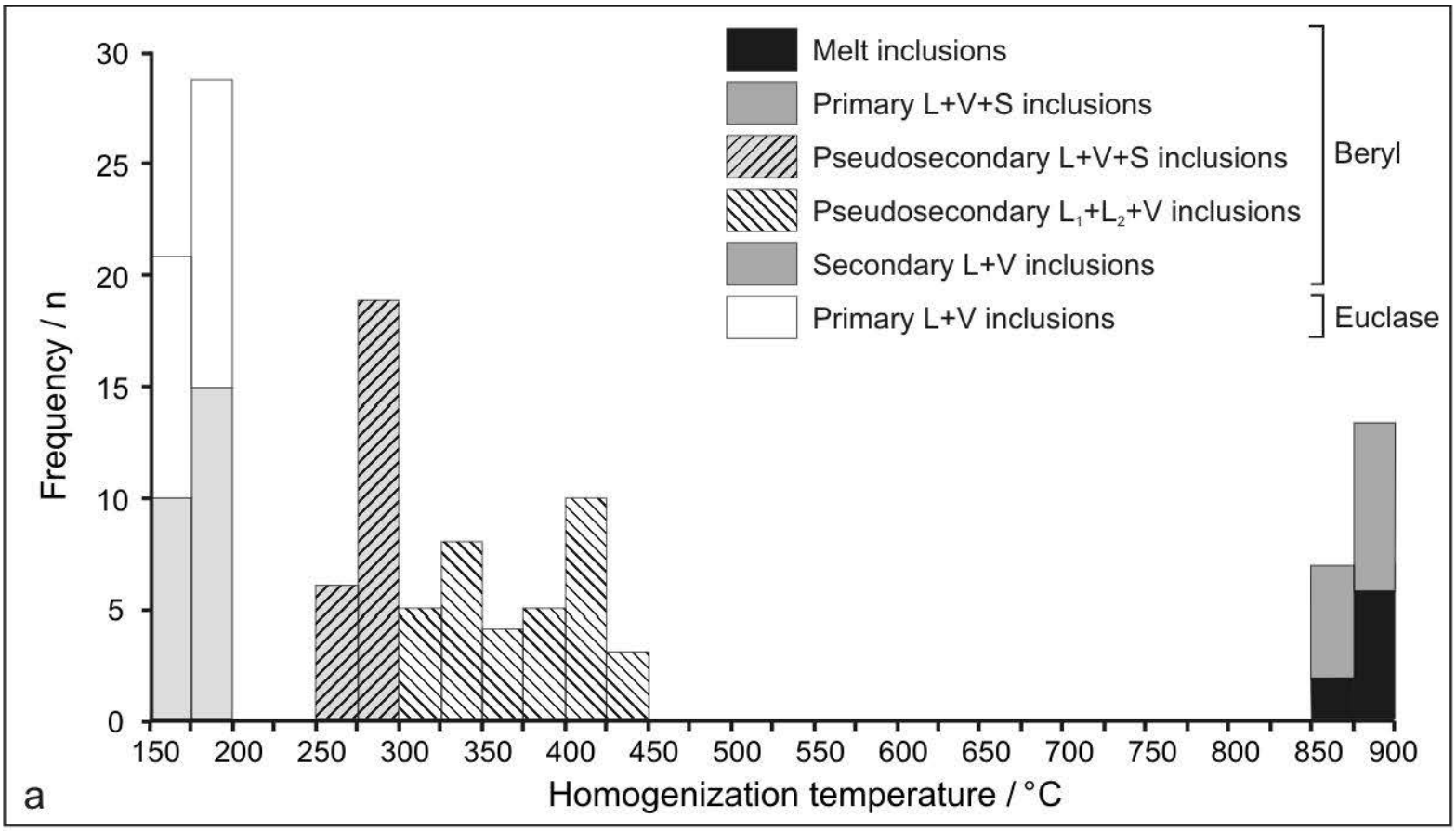
Melt inclusions
Primary L+V+S inclusions
Pseudosecondary L+V+S inclusions
Pseudosecondary L1+L2+V inclusions
Secondary L+V inclusions
Primary L+V inclusions
Beryl
Euclase
Frequency / n
Homogenization temperature / °C
a

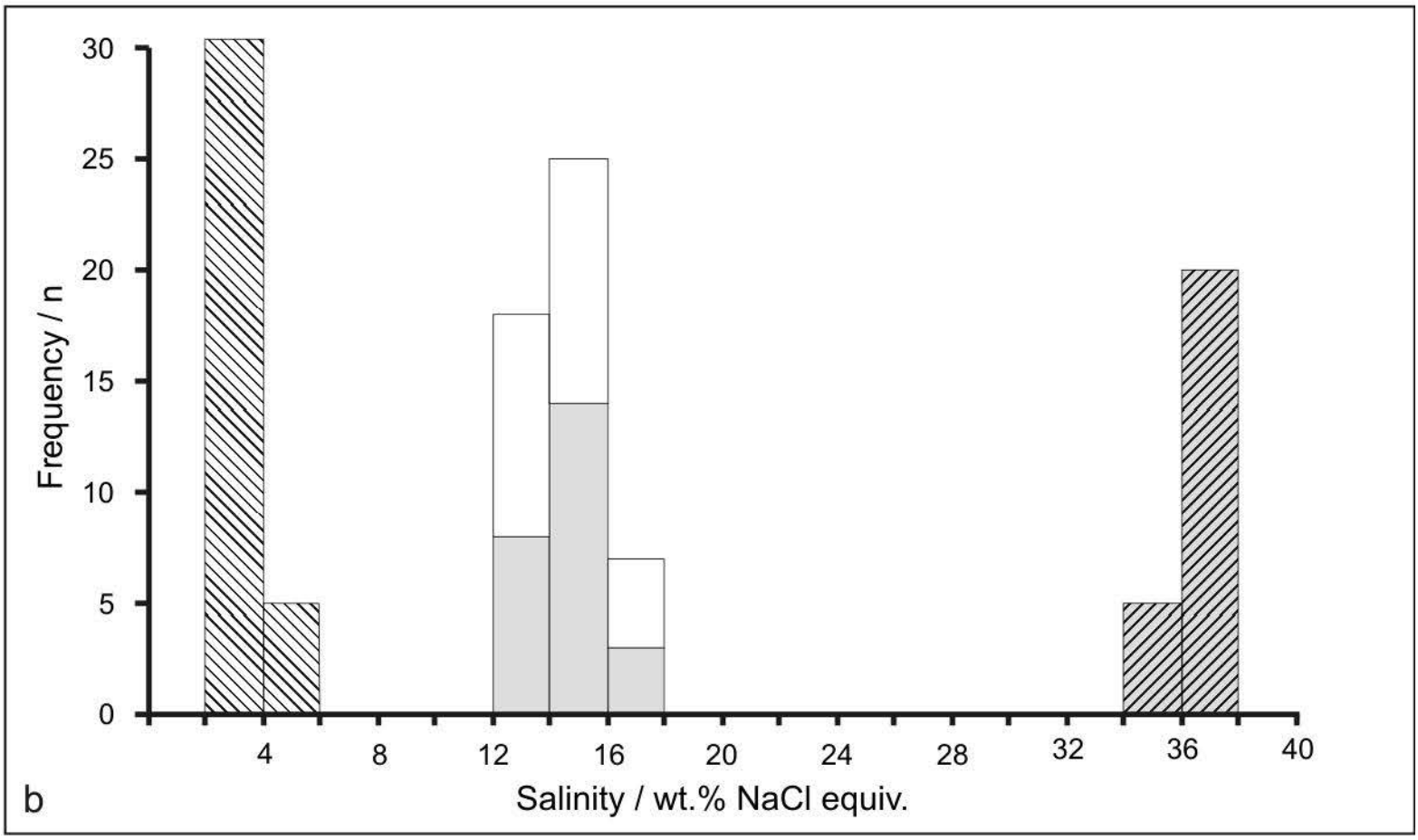
Frequency / n
Salinity / wt.% NaCl equiv.
b

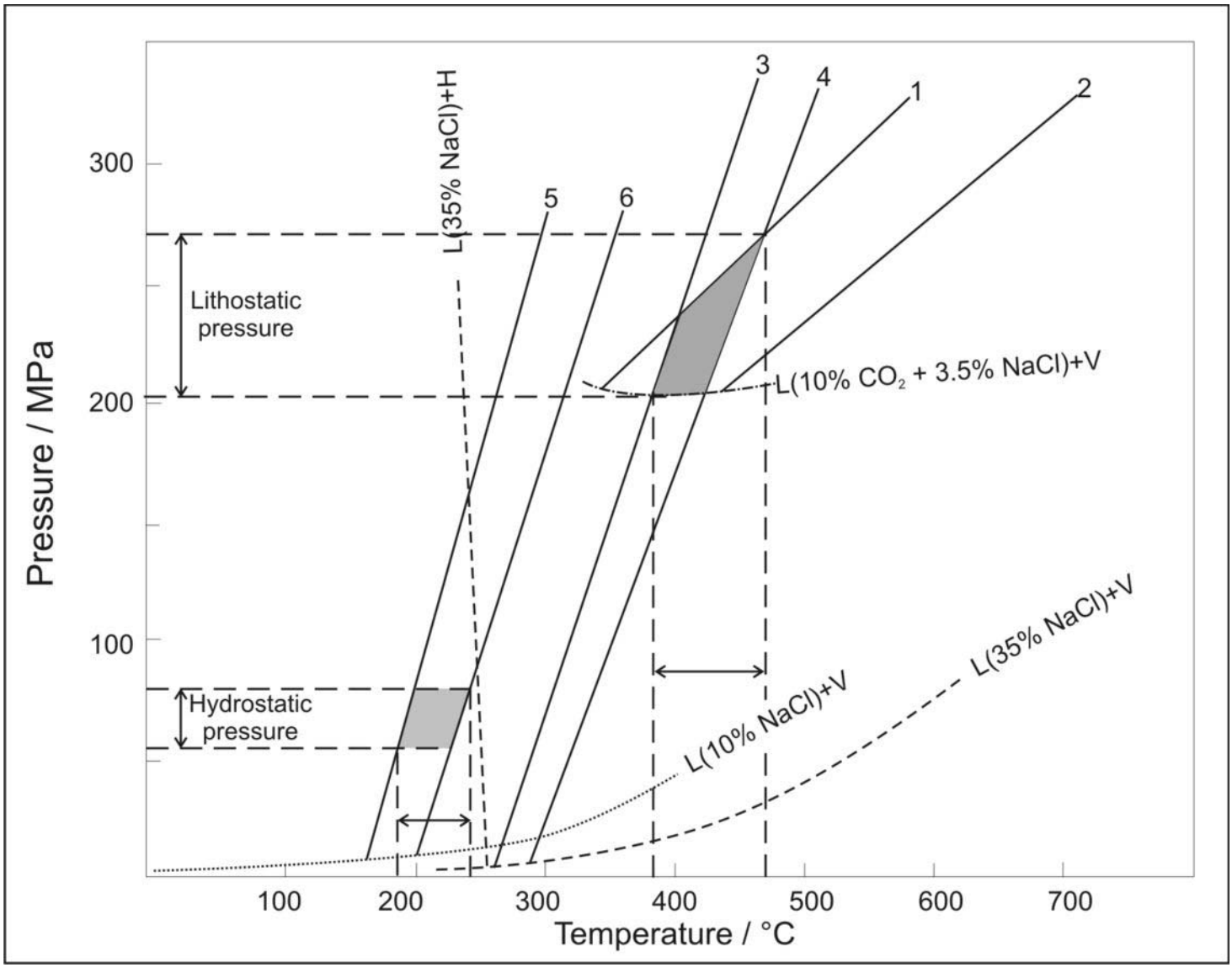
Pressure / MPa
Temperature / °C
300
200
100
100
200
300
400
500
600
700
Lithostatic pressure
Hydrostatic pressure
L(35% NaCl)+H
L(10% CO2 + 3.5% NaCl)+V
L(10% NaCl)+V
L(35% NaCl)+V
1
2
3
4
5
6

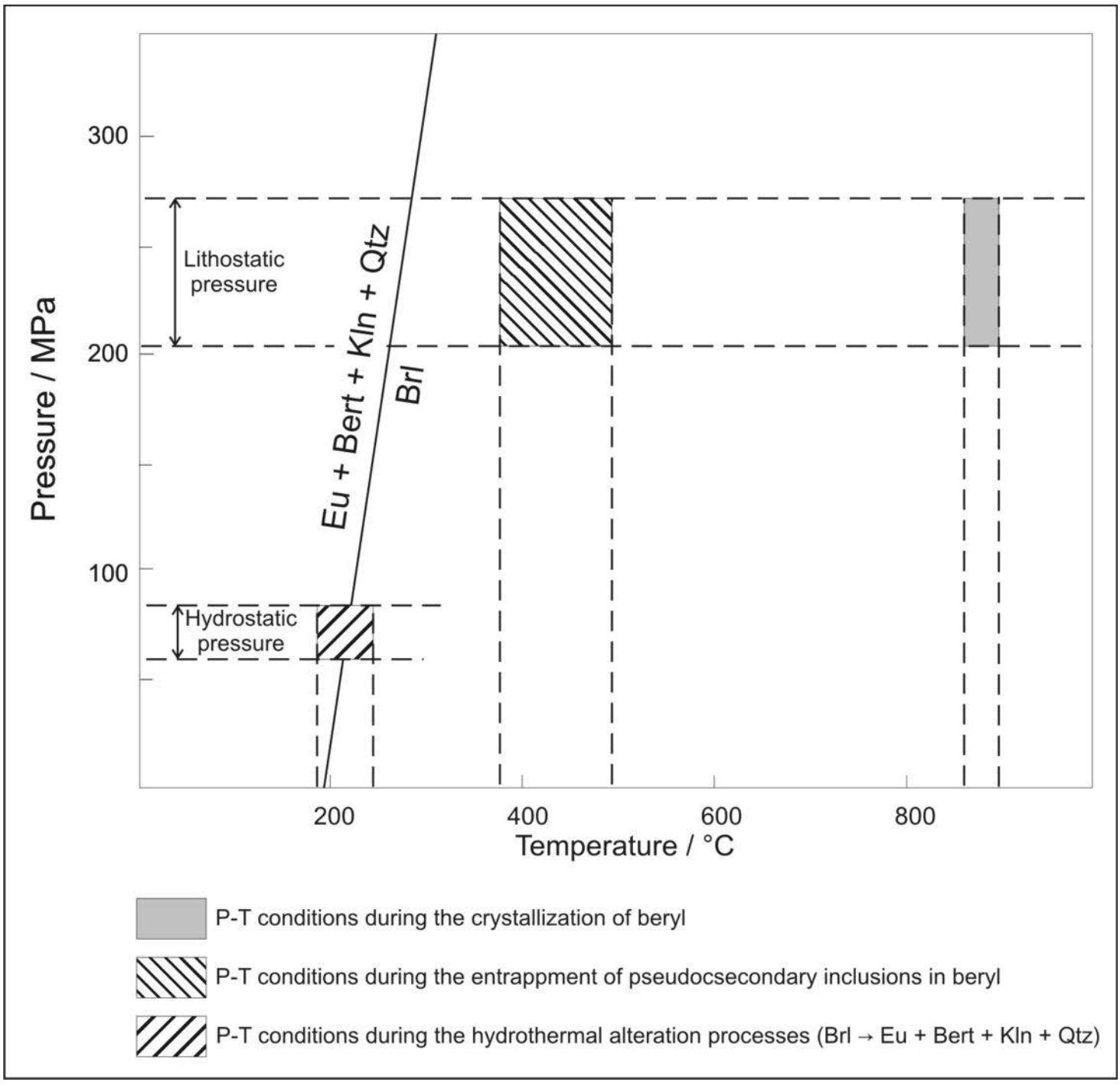
Pressure / MPa
300
200
100
Lithostatic pressure
Hydrostatic pressure
Eu + Bert + Kln + Qtz
Brl
200
400
600
800
Temperature / °C
P-T conditions during the crystallization of beryl
P-T conditions during the entrappment of pseudocsecondary inclusions in beryl
P-T conditions during the hydrothermal alteration processes (Brl → Eu + Bert + Kln + Qtz)